Weakly first-order transition in an athermal lattice gas

Mauro Sellitto*

Dipartimento di Ingegneria, Università degli Studi della Campania "Luigi Vanvitelli", Via Roma 29, 81031 Aversa, Italy and The Abdus Salam International Centre for Theoretical Physics, Strada Costiera 11, 34151 Trieste, Italy

(Received 8 September 2021; revised 18 March 2022; accepted 15 April 2022; published 2 May 2022)

We investigate the phase behavior of a two-dimensional athermal lattice gas in which every hard-core particle can have two or fewer nearest neighboring occupied sites on the square lattice. The ground state and close packing density are determined and it is found that at large chemical potential the model undergoes an ordering phase transition with preferential sublattice occupation. Although near the transition point the particle density and entropy exhibit an apparent discontinuity, we find that the order parameter and fluctuations of thermodynamic quantities do not scale with the system volume. These paradoxical results are reconciled by analyzing the size-dependent flow of the thermal exponent by phenomenological renormalization and the curve-crossing method, which lead to a weakly first-order phase transition scenario.

DOI: 10.1103/PhysRevE.105.054101

I. INTRODUCTION

Lattice models have played and continue to play a vital role in statistical mechanics as a testing ground for the theory of critical phenomena and as a key to the phase behavior of matter. A particularly interesting family includes hard-core lattice gases, i.e., systems of general shaped particles that cannot overlap. In these systems the temperature plays no role because the allowed particle configurations have zero energy, whereas the forbidden ones correspond to an infinite energy state. Consequently, the phase behavior is controlled by purely entropic effects rather than the usual energy-entropy tradeoff of more conventional thermal systems. Paradoxically enough, entropy alone can drive a variety of ordering and self-assembly processes in these athermal systems [1,2], the most prominent example being the isotropic-nematic phase transition of hard rod molecules [3]. Due to the difficulty of disentangling and evaluating the different (translational, rotational, conformational, etc.) entropy contributions, the range of universal critical behaviors encompassed by excluded volume interactions remains only partly explored and there is great interest in engineering entropy for the inverse design of soft matter systems [4]. In this endeavor it is crucial to correctly identify the possible presence of long-range correlations and spontaneously symmetry-broken phases. Although the theoretical distinction between first- and second-order transitions is conceptually clear, this identification is sometime difficult in practice because singular behavior is always rounded and shifted in a finite system by an amount of order $L^{-1/\nu}$, with $\nu = 1/d$ for a first-order transition, d being the spatial dimensionality and L the linear system size.

A subtle and particularly troubling issue occurs when L is comparable to the (generally unknown) correlation length ξ. In this case thermodynamic quantities do not scale with d but rather with nontrivial critical exponents, even though ξ remains finite (i.e., no critical phenomenon is involved) in the thermodynamic limit, $L/\xi \to \infty$. Then, if ξ is sufficiently large the conventional finite-size scaling approach fails to detect the very nature of the phase transition. Weakly first-order transitions are perhaps the most emblematic cases of this situation. They occur, for example, in the isotropic-nematic transition, which is accompanied by remarkable critical properties known as pretransitional effects [5]. They also appear in some quantum magnets, whose behavior is dominated by critical fluctuations, and the true discontinuous nature of the transition is hardly observable with standard experimental methods [6]. The best understood statistical mechanics system is perhaps the two-dimensional Q-state Potts model. It displays a second-order transition for $Q \leqslant 4$ and a first-order transition for $Q > 4$ [7]. However, when $Q = 5$ the correlation length is so large, $\xi \approx 2500$ [8], that the condition $L \gg \xi$ cannot be achieved in any Monte Carlo simulations. It is therefore important to infer unambiguously the precise nature of the phase transition in finite systems by means of systematic extrapolation methods. This can be done by studying the size-dependent flow of critical exponents, and this method has been successfully applied and illustrated with detailed tests to both classical and quantum systems [9–11]. Obviously, depending on the scale L our system is engineered, the mathematical asymptotic limit $L/\xi \to \infty$ may or may not be suitable for describing the actual physical behavior of the system. For example, in the extreme case of bootstrap percolation (for a review, see [12]), a problem which is thought to be relevant to a variety of complex systems, that limit is well beyond the length scales of physical interest.

In this paper we show that a weakly first-order transition occurs in a purely athermal lattice-gas in two spatial dimensions, in which hard-core particles may have *two* or fewer occupied nearest neighbors on the square lattice. This will be denoted henceforth as the BM_2 model because it can be considered a special case of the Biroli-Mézard (BM)

*mauro.sellitto@unicampania.it; mauro.sellitto@gmail.com

model [13], in which every particle may have ℓ or fewer occupied nearest neighbors. The BM_ℓ model interpolates between the nearest neighbor exclusion model [14] with $\ell = 0$, which exhibits a continuous phase transition in the Ising universality class [15,16], and the noninteracting lattice gas, corresponding to $\ell = c$ (with c being the lattice coordination number). From a geometric point of view, this form of excluded volume interaction can be thought of as due the local steric hindrance of molecules having $c - \ell$ arms with the length equal to the lattice spacing. Since the BM model was introduced as a possible three-dimensional realization of the thermodynamic glass transition, it has been especially studied in polydisperse mixtures (with different types of ℓ-particles) and on the Bethe lattice in both classical and quantum domains [17–21], and has inspired a family of various disorder-free lattice models of glassy dynamics [22–25]. Little attention has been paid instead to the phase behavior of the simplest monodisperse case in generic spatial dimension d. To bridge this gap we have begun to address systematically some of these questions which we believe can shed some light on the conditions that determine glass vs crystal formation in more realistic molecular systems. We find, for example, that on the square lattice the BM_3 model exhibits a first-order phase transition, while the phase ordering of the BM_1 model is hindered by the existence of multiple ground states unrelated by a simple symmetry transformation [26].

The layout of the rest of the paper is as follows. The ground-state close packed structure of the BM_2 model and the order parameter definition are discussed in Sec. II. In Sec. III we describe the grand-canonical Monte Carlo algorithm and provide numerical evidence for the existence of a phase transition. In Sec. IV the critical point is located by using the Binder ratio and its size-dependent shift is investigated at phase coexistence. Finite-size scaling of order parameter, susceptibility, and compressibility is addressed in Sec. V. In Sec. VI we analyze the size-dependent flow of the correlation length exponent and show that this makes it possible to detect the signature of weakly first-order transition. Section VII is devoted to some concluding remarks and prospect of future works.

II. GROUND STATE PROPERTIES AND ORDER PARAMETER

The close packing state of the BM_2 model is obtained in the asymptotic limit of infinite chemical potential and has to satisfy the excluded volume condition that the maximum number of particles surrounding any particle is 2. Since there is no explicit constraint on the local geometric structure around an empty site, one can further assume that the maximum number of particles surrounding any vacancy should be 4, if this is compatible with the symmetry of the problem. From these two conditions, starting from a vacancy, one can construct iteratively the crystalline configurations shown in Fig. 1. These can be envisioned as a series of parallel stairs (whose elementary building block is made up of two juxtaposed particles) alternating with a line of vacancies, in the diagonal or antidiagonal directions [Figs. 1(a) and 1(b), respectively]. The two configurations are related by a $\pi/2$ rotation and lead to a natural decomposition of the lattice in three distinct

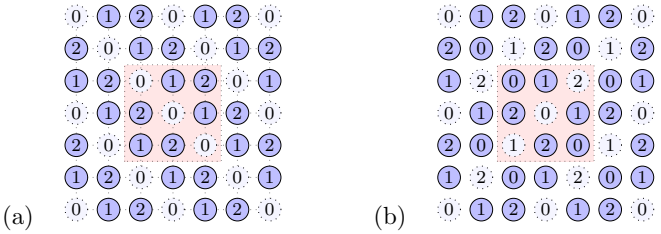

FIG. 1. The two symmetric ground state configurations of the BM_2 model on the square lattice, corresponding to the close packing density $\rho_{\max} = 2/3$. Lattice sites are represented by circles, with filled circles standing for particles and empty circles for vacancies. The central shaded 3×3 square represents the unit cell. For the labeling shown here the density of sublattices $\mathcal{L}_0$, $\mathcal{L}_1$, and $\mathcal{L}_2$, in the ground state configurations is $\rho_0 = 0$, $\rho_1 = \rho_2$ in (a), and $\rho_0 = \rho_1 = \rho_2$ in (b).

sublattices $\mathcal{L}_\alpha$, with $\alpha = 0, 1, 2$, each one having density ρ_α. The close packing density is therefore $\rho_{\max} = 2/3$.

One can easily argue that at low-density, when the excluded volume constraint is negligible, the three sublattices are equally populated, $\rho_0 = \rho_1 = \rho_2$, since there are no extra interactions. At high density, instead, when steric hindrance becomes relevant, ρ_α are unequal, with two sublattices being preferentially occupied and one being preferentially empty. It is therefore reasonable to expect that by increasing the average particle density the system undergoes a phase transition from an isotropic fluidlike phase to a high-density crystalline phase in which the sublattice symmetry is broken. To characterize the two ground state configurations we can attach to the lattice sites two distinct labelings, say A and B. Figure 1 shows one such labeling. By doing so, the ground state configurations for a given labeling are represented in such a way that either one sublattice is empty and the others are fully occupied, as in Fig. 1(a), or all three sublattices are equally populated, as in Fig. 1(b). Since it is unknown *a priori* which labeling is more appropriate to the ground-state configuration the system will choose at high density, the relevant order parameter of the phase transition can be defined as

$$q = \frac{1}{\rho_{\max}} \langle |q_{\mathrm{A}} - q_{\mathrm{B}}| \rangle, \tag{1}$$

where $\langle \cdots \rangle$ is the ensemble average, q_{A} is

$$q_{\mathrm{A}} = \left|\rho_0^{\mathrm{A}} - \rho_1^{\mathrm{A}}\right| + \left|\rho_1^{\mathrm{A}} - \rho_2^{\mathrm{A}}\right| + \left|\rho_2^{\mathrm{A}} - \rho_0^{\mathrm{A}}\right|, \tag{2}$$

and equivalently for the labeling B. Accordingly, in the low-density phase, when all sublattices are equally populated, $q_{\mathrm{A}} = q_{\mathrm{B}} = 0$, we obtain $q = 0$. At high density, when the sublattice symmetry is broken, we have $q > 0$ because either $q_{\mathrm{A}} > 0$, $q_{\mathrm{B}} = 0$, or $q_{\mathrm{A}} = 0$, $q_{\mathrm{B}} > 0$. In the close packed state $q = 1$. Since each of the two ground-state configurations are threefold degenerate (corresponding to the three possible ways the sublattices are occupied by vacancies), the overall degeneracy of the ground state is 6. The analogy with the two-dimensional Potts model, for which the phase transition is first order when the ground-state degeneracy is larger than 4 [7], would suggest that the phase transition of BM_2 model cannot be continuous. Since the correlation length of the six-state Potts model is quite large, $\xi \simeq 159$ [8], it might be difficult to

make $L \gg \xi$ in numerical simulations. If this is so we should expect large corrections to the leading scaling functions and the observation of critical fluctuations on intermediate length scales. To test this prediction more quantitatively we need to look more closely at the nature of the critical point.

III. GRAND-CANONICAL MONTE CARLO AND THERMODYNAMIC EVIDENCE OF PHASE TRANSITION

To investigate the phase behavior of the BM_2 model we perform Monte Carlo (MC) simulations in the grand-canonical ensemble. This offers the advantage of a more efficient sampling of the configuration space when compared to a system with a fixed particle number as the dynamics can indeed more easily escape long-lived metastable states by letting the particles caged by their neighbors to jump into the reservoir. In other words, the reservoir speeds up the particle diffusion by allowing virtual particle motion over longer distances, provided that the reservoir chemical potential is finite. To mimic the interaction of the system with the reservoir an extra bond is added to every lattice site. In a square lattice of side L there will be therefore an overall number of $3L^2$ bonds ($2L^2$ bonds between nearest neighboring sites, plus L^2 bonds to the reservoir). In every Monte Carlo step a bond is randomly selected and, depending on its type, a particle displacement or a particle exchange with the reservoir is attempted. The local excluded volume condition is met whenever particle-diffusion or particle-insertion from the reservoir occurs. In a MC sweep there will occur, on average, a particle exchange with the reservoir for every lattice site, randomly alternating with particle displacements. As the temperature plays no role we set $k_B T = 1$ throughout, and consider changes in the only relevant independent parameters, the volume L^2 and the chemical potential μ of the particle reservoir. Boundary conditions are fully periodic. We first evaluated the particle density ρ by slowly annealing an initial empty system in contact with a particle reservoir from low to high chemical potential with a rate of $\Delta\mu = 10^{-2}$ per 10^5 MC sweeps. The entropy s was then obtained by using the thermodynamic integration method, $s(\mu_f) = s(\mu_i) - \int_{\mu_i}^{\mu_f} \mu \, d\rho$, with μ_i chosen sufficiently low as to make the excluded volume interaction ineffective [so that the $s(\mu_i)$ coincides with the entropy of the noninteracting lattice gas]. In Fig. 2 we show a plot of curves $\rho(\mu)$ and $s(\mu)$. These quantities are compared with those of the noninteracting lattice gas, for which $\rho(\mu) = 1/[1 + \exp(-\mu)]$ and $s(\mu) = -\rho(\mu)\ln\rho(\mu) - [1 - \rho(\mu)]\ln[1 - \rho(\mu)]$. As anticipated above, the two systems display the same thermodynamics at low density, as long as $\rho < 0.2$ ($\mu < -1.5$). Increasing the chemical potential, the two curves depart from one another, meaning that the excluded volume interaction becomes more and more effective. In the range $\mu \in [2.84, 2.87]$ we observe a sudden jump in both density and entropy, which clearly suggests the existence of a first-order phase transition. Interestingly, the analysis of the cavity equations on the corresponding Bethe lattice, namely the random regular graph with connectivity equal to 4 [17], shows that the entire fluid phase is well described by the factorized replica symmetric solution—see dotted blue line in Fig. 2—with a slight discrepancy occurring only near

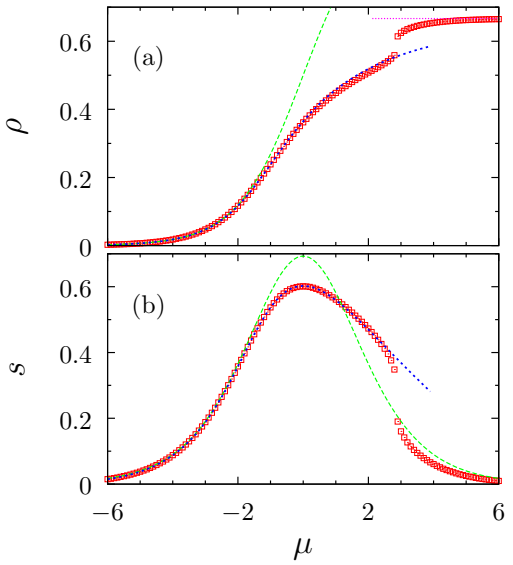

FIG. 2. Thermodynamic properties of the two-dimensional BM_2 model on the square lattice. Data points (square symbols), extracted from grand-canonical Monte Carlo simulation of a system of linear size $L = 75$, are compared with the noninteracting lattice gas behavior (dashed curve) and the Bethe-Peierls, or replica factorized, approximation (dotted curve). (a) Particle density ρ vs chemical potential μ. The horizontal segment indicates the close packing density $\rho_{\max} = 2/3$. (b) Entropy s vs chemical potential μ. The phase transition is located in the range $\mu \in [2.84, 2.87]$.

the phase transition. Further increasing the chemical potential eventually leads the system to attain the previously computed closest packing density, $\rho_{\max} = 2/3$. In this limit the system entropy vanishes, consistently with the finite (system-size independent) degeneracy of the ground state.

IV. BINDER RATIO AND PHASE COEXISTENCE

To locate more precisely the critical point and get a first insight into the microscopic nature of the phase transition we study the Binder ratio U_L of the order parameter probability density function [27]. Here we find it convenient to define U_L as

$$U_L(\mu) = \frac{1}{2}\left(\frac{\langle q^4\rangle}{\langle q^2\rangle^2} - 1\right), \tag{3}$$

where $\langle q^k\rangle$ is the k-order cumulant of the order-parameter distribution $P_L(q, \mu)$. Accordingly, we expect that in the low density fluidlike phase $U_L \to 1$ [assuming a Gaussian $P_L(q, \mu)$, and therefore $\langle q^4\rangle = 3\langle q^2\rangle$], while in the high density solidlike phase $U_L \to 0$ (assuming a Dirac delta order-parameter distribution, and thus $\langle q^k\rangle = \langle q\rangle^k$). Assuming that near the critical point the growing correlation length leaves the system scale invariant, one can argue that $\langle q^k\rangle = L^{-k\beta/\nu}\mathcal{Q}_k[(\mu_c - \mu)L^{1/\nu}]$, where $\mathcal{Q}_k$ is a scaling function, β is the order parameter exponent, and ν the correlation length exponent. We thus expect that the Binder ratio scales asymptotically as

$$U_L(\mu) = \mathcal{U}[(\mu_c - \mu)L^{1/\nu}], \tag{4}$$

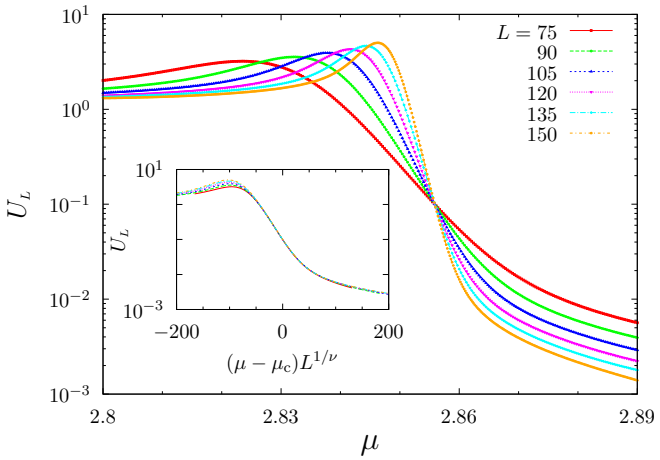

FIG. 3. Binder ratio U_L vs chemical potential μ in the two-dimensional BM_2 model on the square lattice of side L. The crossing point is approximately located at $\mu_c = 2.8559(1)$. The peaks location shifts from left to right with increasing L. Inset: Binder ratio vs scaled distance to the critical point with $\nu = 0.54$ and $\mu_c = 2.8559$.

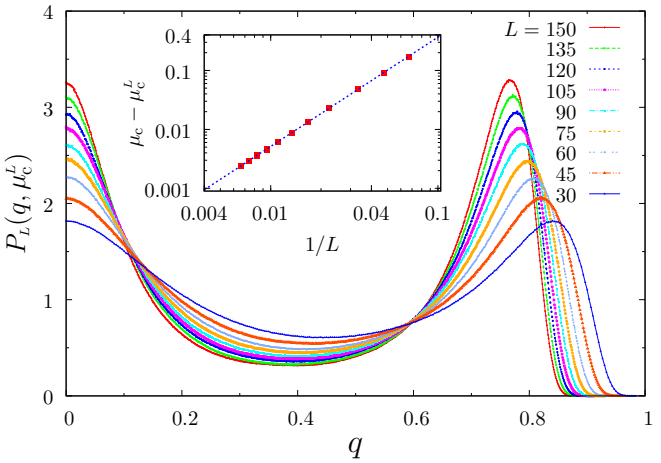

FIG. 4. Finite-size probability density function $P_L(\mu, q)$ of the order parameter q evaluated at the chemical potential μ_c^L at which the peaks have equal height (L is the square lattice side; larger values of L correspond to higher peaks). Inset: power-law fit of the finite-size shifted critical point $\mu_c - \mu_c^L$ vs inverse length $1/L$. The estimated value of the infinite volume limit of the critical point and the correlation length exponent are $\mu_c = 2.8559(1)$ and $\nu = 0.54(1)$, respectively.

where $\mathcal{U}$ is a scaling function. This implies that a sensible estimation of the critical chemical potential μ_c can be obtained by looking at the crossing point of $U_L(\mu)$ for different system sizes, while the data collapse of U_L plotted vs the scaled distance to the critical point gives the possibility of estimating ν. We evaluated the Binder ratio throughout the critical region from time series of long MC runs, typically 10^8 MC sweeps, by means of the histogram reweighting technique [28–30]. Results were averaged over ten realizations of the random noise, after the system was aged in the critical region for an extra time of about 10^6–10^8 MC sweeps. Thermalization was checked by looking at the time-translation invariance of the two-time density-density correlation function. Figure 3 shows $U_L(\mu)$ curves on a semilogarithmic scale for linear system size L in the range [75,150]. The intersection of the different curves allows one to locate the critical point at $\mu_c = 2.8559(1)$. Three distinctive features of the Binder ratio can be observed in Fig. 3: (i) U_L is a nonmonotonic function of μ, (ii) it displays a peak that grows and sharpens with L, and (iii) its logarithm behaves linearly over a critical region that shrinks with L. These features are rather different than those expected from the Ising model and other systems with continuous phase transitions, where instead U_L typically stays bounded and tends to a step function monotonically. Indeed, the above features are due to the emergence of multiple peaks in the order-parameter distribution and are thus generally taken as a signature of phase coexistence, i.e., that the transition is of first order [11,31–33]. Nevertheless, it should be emphasized that multiple peaks can also appear in some systems with continuous phase transitions such as the Baxter-Wu model, the two-dimensional three- and four-state Potts models, the Ashkin-Teller model, the Ising model with both nearest- and next-nearest-neighbor interactions, and some quantum magnets related to the phenomenon of deconfined quantum criticality [9–11,34–36]. The inset of Fig. 3 shows the Binder ratio plotted against the scaled distance to the critical point for various system sizes. As expected for a first-order phase transition we find a good data collapse only in a linear (on a semilogarithmic scale) region around the critical point, with $\nu = 1/2$. However, a good data collapse over a larger scaling window beyond the linear region is obtained also with $\nu = 0.54$, although significant size dependence remains in the neighborhood of the peak. So, to further understand the nature of the phase transitions, we sought phase coexistence and finite-size corrections to the critical point. We observe that in the critical region the order-parameter distribution $P_L(q, \mu)$ develops in fact a pronounced double-peak structure corresponding to the simultaneous formation of two distinct phases near the transition point: one is located at $q = 0$ and corresponding to the disordered fluidlike state, while the other is at $q > 0$ in the solidlike ordered state. Figure 4 shows $P_L(q, \mu)$ for L in the range [30,150] at the chemical potential $\mu = \mu_c^L$ at which the two peaks of P_L are of equal height. We will take μ_c^L as our measure of the finite-size shift of the critical point. In spite of the manifest phase coexistence, we see in the inset of Fig. 4 that a power-law fit describes very well the data of μ_c^L with values of ν and μ_c compatible with those obtained with the analysis of the Binder ratio.

V. FINITE-SIZE SCALING AND PSEUDOCRITICAL EXPONENTS

Since the estimated value of the correlation length exponent, $\nu = 0.54$ is sensibly different from that expected for a first-order phase transition ($\nu = 1/2$), we now look at the finite-size scaling behavior of the order parameter q, susceptibility χ,

$$\chi = L^2(\langle q^2 \rangle - \langle q \rangle^2), \tag{5}$$

which describes the mean-squared fluctuations of the order parameter, and compressibility κ,

$$\kappa = \frac{L^2}{\langle\rho\rangle^2}(\langle\rho^2\rangle - \langle\rho\rangle^2), \tag{6}$$

which describes the mean-squared fluctuations of the particle density. Notice that compressibility plays the role of specific heat (the second derivative of free energy with the respect to temperature), because in purely hard-core lattice gases, such as the BM_2 considered here, there is no energy and no temperature. Likewise, density fluctuations are the direct analog of energy fluctuations. Therefore, the critical exponent α is associated with compressibility (the second derivative of entropy with the respect to the control parameter μ). The scaling hypothesis suggests that for a continuous phase transition the above quantities behave as

$$q = L^{-\beta/\nu}\mathcal{Q}[(\mu-\mu_c)L^{1/\nu}], \tag{7}$$

$$\chi = L^{\gamma/\nu}\mathcal{X}[(\mu-\mu_c)L^{1/\nu}], \tag{8}$$

$$\kappa = L^{\alpha/\nu}\mathcal{K}[(\mu-\mu_c)L^{1/\nu}], \tag{9}$$

where $\mathcal{Q}$, $\mathcal{X}$, and $\mathcal{K}$ are scaling functions and the critical exponents β, γ, and α, which characterize the universality class of the phase transition, satisfy the scaling and hyperscaling relations $\alpha + 2\beta + \gamma = 2$ and $2\beta + \gamma = d\nu$, the space dimensionality being d. At a first-order transition instead the relevant scaling is with the volume of the system [37], thus Eqs. (7), (8), and (9) hold with trivial value of critical exponents, $\alpha = 1$, $\beta = 0$, $\gamma = 1$, $\nu = 1/d$. Panels (a), (b), and (c) of Fig. 5 show q, χ, and κ, respectively, in the critical region of chemical potential for linear system sizes L in the range [75, 150]. The inset of each panel of Fig. 5 shows rescaled data with $\alpha = 0.85(2)$, $\beta = 0.04(1)$, $\gamma = 1.10(4)$, and the previously estimated $\mu_c = 2.8559(1)$, and $\nu = 0.54(1)$. The data collapse is so successful that would seem to suggest, rather convincingly, a continuous phase transition with nontrivial values of the critical exponents, if we did not know from Sec. III the true first-order nature of the transition. The estimated critical exponents are indeed compatible, within the numerical accuracy, with the scaling and hyperscaling relations $\alpha + 2\beta + \gamma = 2$ and $2\beta + \gamma = 2\nu$. Interestingly, they are also very close to those of the universality class of the tricritical Ising model in two dimensions (or, equivalently, the two-dimensional two-state Potts lattice gas) [38], and can be exactly determined from conformal invariance as $\alpha = 8/9$, $\beta = 1/24$, $\gamma = 37/36$, $\nu = 5/9$ [39–41]. A possible justification of this similarity will be suggested in Sec. VII. The way out of this paradox is that we are indeed probing the preasymptotic regime which is still too far from the limit $L \gg \xi$ to show deviations from conventional critical behavior.

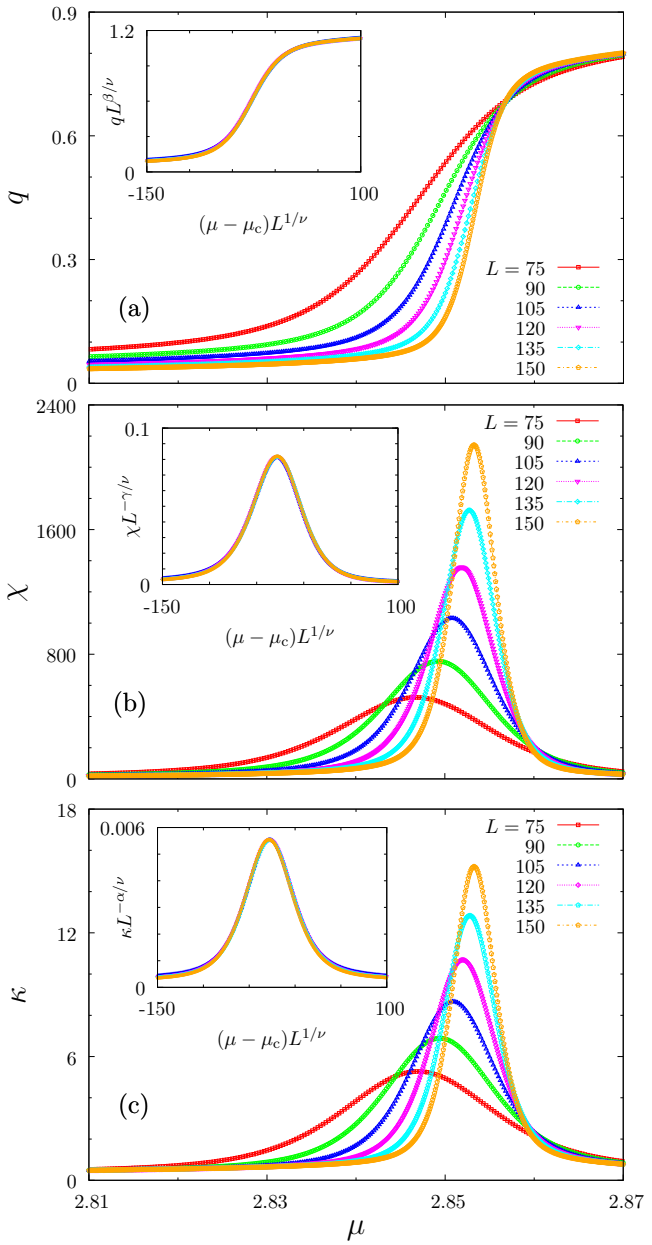

FIG. 5. Finite-size scaling properties of the BM_2 model on a square lattice of side L for (a) order parameter q, (b) susceptibility χ, and (c) compressibility κ vs chemical potential μ, and rescaled data in the inset. In panel (a) larger values of L correspond to steeper curves. In both panels (b) and (c) larger values of L correspond to higher peaks. The values of critical point and critical exponents are $\mu_c = 2.8559$, $\nu = 0.54$, $\beta = 0.04$, $\gamma = 1.1$, and $\alpha = 0.85$. Rescaled data are limited to the four largest sizes, $L > 90$.

VI. CURVE CROSSING METHOD

To corroborate the weakly first-order scenario we next study the size-dependent flow of the correlation length exponent by exploiting phenomenological renormalization [42–44] and the curve-crossing method [10,11]. We here follow the same procedure detailed in Refs. [10,11] and show that it allows one to detect unambiguously the signature of the first-order transition. In the phenomenological renormalization, one considers a dimensionless quantity, for which curves plotted versus the control parameter (here the chemical potential) for two different system sizes, say $L/2$ and L, will cross each other at a point approaching the phase transition point as the system sizes are taken to infinity, and a corresponding critical value of the dimensionless quantity is approached in the vertical direction. The flows of the horizontal and vertical

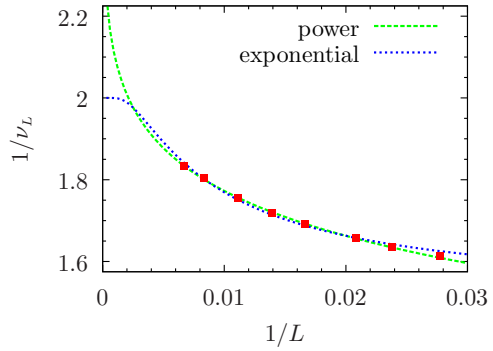

FIG. 6. Size-dependent flow of the inverse correlation-length exponent $1/\nu_L$ at length scale L for the BM_2 model on the square lattice. Squares represent the data obtained from the crossing point analysis with system-size pairs $(L/2, L)$. The dashed green curve is a three-parameter power-law fit, $1/\nu_L = 1/\nu_\infty + a\,L^{-\omega}$, where the effective correction-to-scaling exponent is $\omega \simeq 0.07$ and the extrapolated value $1/\nu_\infty \simeq 3.96$. The dotted blue curve is a two-parameter exponential-law fit $1/\nu_L = 2 + b\exp(-L/\xi)$, where the estimated correlation length is $\xi \simeq 132$. The smallest size was excluded from the fits.

crossing values, as well as the slopes at the crossing points, are governed by the exponent ν and corrections to scaling (the subleading exponent ω). Strong indications of weakly first-order behavior can be detected in the extrapolation of the effective critical exponents in terms of the system size. This is most clearly manifested in the inverse correlation length exponent $1/\nu$ [11], which in the renormalization group approach is known as the thermal eigenvalue (of renormalization group transformations). For this reason we essentially focus on $1/\nu$ and consider for the dimensionless quantity the logarithm of the Binder ratio U_L previously defined in Eq. (3). In practice, we first evaluate $\ln U_L$ on a dense grid of chemical potentials and system sizes. Then, we use polynomial fits for interpolation to obtain the crossing points for system sizes $(L/2, L)$ as well as the slopes at the crossing point. The polynomial fitting is better behaved with the quantity $\ln U_L(\mu)$, which is linear near the transition point [11], as we have seen in the Fig. 3 of Sec. III. The correlation length exponent at the scale L is then extracted as

$$\frac{1}{\nu_L} = \log_2 \left[\frac{\frac{d}{d\mu} \ln U_L(\mu)}{\frac{d}{d\mu} \ln U_{L/2}(\mu)} \right]_{\mu=\mu_{\rm cross}} \tag{10}$$

with $\mu_{\rm cross}$ corresponding to the crossing point of the curves $\ln U_L(\mu)$ and $\ln U_{L/2}(\mu)$, which are computed, along with their derivatives, from the fitted polynomials. In Fig. 6, we show the size-dependent exponent $1/\nu_L$ of the BM_2 model obtained from the crossing point method. The next step of the analysis proceeds by a classical *reductio ad absurdum*. We assume the transition is continuous and therefore a power-law finite-size correction $L^{-\omega}$ to the leading scaling form Eq. (4). If any inconsistency on the flow of $1/\nu_L$ toward the asymptotic value results from this assumption then the phase transition cannot be continuous. The dashed line in Fig. 6 shows in fact that a power-law form yields a very good fit of $1/\nu_L$ data. However, this requires an anomalously small subleading correction exponent, $\omega \simeq 0.07$. Further, the extrapolated value $1/\nu_\infty \simeq 3.96$ far exceeds the first-order value 2 and the previously estimated $1/\nu \simeq 1/0.54 \simeq 1.85$, while at a continuous transition it should never be larger than d (d being the spatial dimension). Therefore, a continuous phase transition is untenable. In contrast, if we assume that the transition is first order we can see that the data for $1/\nu_L$ are described as well by an exponentially rapidly approach to the asymptotic value $1/\nu = 2$ over the same range of system sizes (dotted line in Fig. 6). Several interesting features emerge from the comparison of the exponential and power law forms. First, the two forms agree over an extended range of system sizes which goes quite beyond the available data set of $1/\nu_L$ (up to $L \approx 500$). Second, the smallest system size that would be required to clearly distinguish between the two forms is about $L \approx 800$, which is quite beyond what we could afford. Third, the correlation length extracted from the exponential fit, $\xi \simeq 132$, is comparable with that of the six-state Potts model, $\xi \simeq 159$ [8], which is consistent with the ground state degeneracy of the BM_2 model, as pointed out in Sec. II. This definitely confirms the weakly first-order character of the phase transition, even though it is not possible to reach the system sizes over which the crossover from second- to first-order scaling is manifestly evident. Therefore we can conclude that the nontrivial critical behavior observed in Secs. IV and V represents a large preasymptotic effect.

VII. CONCLUSIONS AND PERSPECTIVES

We have studied the phase behavior of a two-dimensional Biroli-Mézard model in which every particle can have two or fewer nearest neighboring occupied sites on the square lattice. We have determined the structure of the ground state and the close packed density and showed that the system undergoes an ordering transition from a dilute fluidlike phase to a solidlike phase in which the sublattice symmetry is broken. The transition is of first order because the particle density and entropy display a sudden jump at a critical chemical potential that we identify by studying the Binder ratio. The analysis of the probability density function of the order parameter has made evident that near the critical point the system exhibits phase coexistence. Thermodynamic observables, however, do not scale simply with the system volume. Rather, they exhibit nontrivial critical exponents, that we have identified via finite-size scaling analysis and the histogram reweighting technique. We have thus seen that conventional finite-size scaling fails to detect unambiguously the weakly first-order character of the phase transition, which is instead correctly captured by the extrapolation of the size-dependent flow of the thermal exponent, which we have obtained via the crossing point method.

We believe that the nontrivial critical behavior observed here in the preasymptotic regime, and which is manifested in critical exponents close to the universality class of the two-dimensional tricritical Ising model, provides a strong indication of the presence of a tricritical point in the global phase diagram of the BM_2 model in which suitable extra diagonal interactions are introduced. In this case, one of the two ground state configurations becomes unstable, and thus the ground state degeneracy is reduced from 6 to 3. The analogy with the Potts model thus suggests that the modified system belongs to the universality class of the two-dimensional dilute

Potts lattice gas. This scenario is made plausible by the fact that a similar situation occurs in the square lattice gas with diagonal interactions [45–47]. A changeover from first- to second-order transition via a tricritical point should be also expected for mixtures of particles with different types of excluded volume interactions, in analogy with the results of Refs. [48–51]. It is known that the nature of the phase transition displayed by extended hard-core lattice gases, which has been much studied in the past decades [52–61], depends sensitively on the underlying lattice structure and the precise extension of the short-range exclusion. This goes against the conventional wisdom of renormalization group approach and in this respect, the prospect of extending to higher-order neighbors the range of the excluded volume interaction in the BM model would be very interesting, also because it provides a way to approach the continuum limit of a fluid made of general shaped particles. Finally, the reformulation of the BM model in terms of known statistical mechanics models, such as the Coulomb gas or vertex models, might give the possibility of exploiting analytical techniques for deriving some exact results [62,63].

ACKNOWLEDGMENTS

It is a pleasure to thank R. Fazio and M. Kiselev for the kind hospitality in the Condensed Matter and Statistical Physics Section of ICTP (Trieste, IT). Numerical simulations were performed by using ICTP computer facilities.

[1] D. Frenkel, Nat. Mater. **14**, 9 (2015).
[2] G. M. Whitesides and B. Grzybowski, Science **295**, 2418 (2002)
[3] L. Onsager, Ann. N. Y. Acad. Sci. **51**, 627 (1949).
[4] F. A. Escobedo, Soft Matter **10**, 8388 (2014).
[5] P.-G. de Gennes and J. Prost, *The Physics of Liquid Crystals* (Oxford University Press, Oxford, 1993).
[6] Y. Kamiya, N. Kawashima, and C. D. Batista, Phys. Rev. B **82**, 054426 (2010).
[7] R. J. Baxter, J. Phys. C: Solid State Phys. **6**, L445 (1973).
[8] E. Buddenoir and S. Wallon, J. Phys. A: Math. Gen. **26**, 3045 (1993).
[9] S. Jin, A. Sen, and A. W. Sandvik, Phys. Rev. Lett. **108**, 045702 (2012).
[10] H. Shao, W. Guo, and A. W. Sandvik, Science **352**, 213 (2016).
[11] S. Iino, S. Morita, N. Kawashima, and A. W. Sandvik, J. Phys. Soc. Jpn. **88**, 034006 (2019).
[12] P. De Gregorio, A. Lawlor, and K. A. Dawson, in *Encyclopedia of Complexity and Systems Science*, edited by R. A. Meyers (Springer, Berlin, 2009), pp. 608–626.
[13] G. Biroli and M. Mézard, Phys. Rev. Lett. **88**, 025501 (2001).
[14] D. S. Gaunt and M. E. Fisher, J. Chem. Phys. **43**, 2840 (1965).
[15] G. Kamieniarz and H. W. J. Blöte, J. Phys. A: Math. Gen. **26**, 6679 (1993).
[16] W. Guo and H. W. J. Blöte, Phys. Rev. E **66**, 046140 (2002).
[17] O. Rivoire, G. Biroli, O. C. Martin, and M. Mézard, Eur. Phys. J. B **37**, 55 (2004).
[18] K. A. Dawson, S. Franz, and M. Sellitto, Europhys. Lett. **64**, 302 (2003).
[19] E. Marinari and V. Van Kerrebroeck, Europhys. Lett. **73**, 383 (2006).
[20] R. K. Darst, D. R. Reichman, and G. Biroli, J. Chem. Phys. **132**, 044510 (2010).
[21] L. Foini, G. Semerjian, and F. Zamponi, Phys. Rev. B **83**, 094513 (2011).
[22] M. P. Ciamarra, M. Tarzia, A. de Candia, and A. Coniglio, Phys. Rev. E **67**, 057105 (2003).
[23] M. Weigt and A. K. Hartmann, Europhys. Lett. **62**, 533 (2003).
[24] G. D. McCullagh, D. Cellai, A. Lawlor, and K. A. Dawson, Phys. Rev. E **71**, 030102(R) (2005).
[25] F. Krzakala, M. Tarzia, and L. Zdeborová, Phys. Rev. Lett. **101**, 165702 (2008).
[26] M. Sellitto, J. Chem. Phys. **156**, 124105 (2022); and (unpublished).
[27] K. Binder, Z. Phys. B **43**, 119 (1981).
[28] A. M. Ferrenberg and R. H. Swendsen, Phys. Rev. Lett. **61**, 2635 (1988).
[29] M. Newman and G. Barkema, *Monte Carlo Methods in Statistical Physics* (Oxford University Press, New York, 1999).
[30] W. Janke, in *Ageing and the Glass Transition*, edited by M. Henkel, M. Pleiming, and R. Sanctuary (Springer-Verlag, Berlin, 2007), pp. 207–260.
[31] K. Binder and D. P. Landau, Phys. Rev. B **30**, 1477 (1984).
[32] P. Peczak and D. P. Landau, Phys. Rev. B **39**, 11932 (1989).
[33] K. Vollmayr, J. D. Reger, M. Scheucher, and K. Binder, Z. Phys. B **91**, 113 (1993).
[34] N. Schreiber and J. Adler, J. Phys. A: Math. Gen. **38**, 7253 (2005).
[35] K. S. D. Beach, F. Alet, M. Mambrini, and S. Capponi, Phys. Rev. B **80**, 184401 (2009).
[36] R. K. Kaul, Phys. Rev. B **84**, 054407 (2011).
[37] M. E. Fisher and A. N. Berker, Phys. Rev. B **26**, 2507 (1982).
[38] D. P. Landau and R. H. Swendsen, Phys. Rev. Lett. **46**, 1437 (1981).
[39] B. Nienhuis, J. Phys. A: Math. Gen. **15**, 199 (1982).
[40] A. A. Belavin, A. M. Polyakov, and A. B. Zamolodchikov, J. Stat. Phys. **34**, 763 (1984).
[41] D. Friedan, Z. Qiu, and S. Shenker, Phys. Rev. Lett. **52**, 1575 (1984).
[42] M. E. Fisher, in *Critical Phenomena*, Proceedings of the Enrico Fermi International School of Physics, edited by M. S. Green (Academic, New York, 1971), Vol. 51.
[43] M. N. Barber, in *Phase Transitions and Critical Phenomena*, edited by C. Domb (Academic, New York, 1983), Vol. 8.
[44] J. M. Luck, Phys. Rev. B **31**, 3069 (1985).
[45] R. J. Baxter, J. Phys. A: Math. Gen. **13**, L61 (1980).
[46] D. A. Huse, Phys. Rev. Lett. **49**, 1121 (1982).
[47] R. J. Baxter and P. A. Pearce, J. Phys. A: Math. Gen. **16**, 2239 (1983).
[48] M. W. Springgate and D. Poland, Phys. Rev. A **20**, 1267 (1979).
[49] D. Poland, J. Chem. Phys. **80**, 2767 (1984).
[50] T. J. Oliveira and J. F. Stilck, J. Chem. Phys. **135**, 184502 (2011).
[51] T. J. Oliveira and J. F. Stilck, Phys. Rev. E **92**, 032101 (2015).

[52] L. K. Runnels, in *Phase Transitions and Critical Phenomena*, edited by C. Domb and M. S. Green (Academic, London, 1972), Vol. 2.
[53] S. Prestipino, Phys. Rev. E **62**, 2177 (2000).
[54] L. Lafuente and J. A. Cuesta, Phys. Rev. E **68**, 066120 (2003).
[55] A. Z. Panagiotopoulos, J. Chem. Phys. **123**, 104504 (2005).
[56] H. C. M. Fernandes, Y. Levin, and J. J. Arenzon, J. Chem. Phys. **126**, 114508 (2007).
[57] X. Feng, H. W. J. Blöte, and B. Nienhuis, Phys. Rev. E **83**, 061153 (2011).
[58] K. Ramola and D. Dhar, Phys. Rev. E **86**, 031135 (2012).
[59] T. Nath and R. Rajesh, Phys. Rev. E **90**, 012120 (2014).
[60] T. Nath and R. Rajesh, J. Stat. Mech. (2016) 073203.
[61] F. C. Thewes and H. C. M. Fernandes, Phys. Rev. E **101**, 062138 (2020).
[62] R. J. Baxter, *Exactly Solved Models Statistical in Mechanics* (Academic, London, 1982).
[63] B. Nienhuis, in *Phase Transitions and Critical Phenomena*, edited by C. Domb and J. Lebowitz (Academic, London, 1987), Vol. 11.